Science Advances

AAAS

advances.sciencemag.org/cgi/content/full/3/7/e1700300/DC1

Supplementary Materials for

Urbanization-induced population migration has reduced ambient $PM_{2.5}$ concentrations in China

Huizhong Shen, Shu Tao, Yilin Chen, Philippe Ciais, Burak Güneralp, Muye Ru, Qirui Zhong, Xiao Yun, Xi Zhu, Tianbo Huang, Wei Tao, Yuanchen Chen, Bengang Li, Xilong Wang, Wenxin Liu, Junfeng Liu, Shuqing Zhao

Published 19 July 2017, *Sci. Adv.* **3**, e1700300 (2017)
DOI: 10.1126/sciadv.1700300

The PDF file includes:

- fig. S7. Modeled annual average near-surface $PM_{2.5}$ concentrations in the modeling domain in 2010.
- fig. S8. Comparison of annual average $PM_{2.5}$ concentrations between simulation and observation.
- fig. S9. Comparison of time series of $PM_{2.5}$ concentrations between simulation and observation in Beijing and Shanghai.
- fig. S10. The influences of individual non–migration-related (N1 to N4) and migration-related (U1 to U5) factors on $PM_{2.5}$ emissions in China during the study period.
- fig. S11. Temporal trends of the national total urban area defined by administrative boundaries (*45*) and the built-up area derived in this study.
- References (*63–65*)

Other Supplementary Material for this manuscript includes the following:
(available at advances.sciencemag.org/cgi/content/full/3/7/e1700300/DC1)

- data file S1 (.rar format). Geographic distributions of urban areas in China in 1980, 1990, 2000, 2010, and 2030.
- data file S2 (.rar format). Geographic distributions of the population in China in 1980, 1990, 2000, 2010, and 2030.

Supplementary Materials

Supplementary Methods

Intercalibration of NL data

For NL data, we used the Defense Meteorological Satellite Program's Operational Line-scan System (DMSP-OLS) Nighttime Lights Time Series dataset (*33*). The DMSP-OLS archives annual NL data recorded by six satellites, including F10, F12, F14, F15, F16, and F18, covering the time series from 1992 to 2012 (table S7). The product covers -180° to 180° longitude and -65° to 75° latitude with a spatial resolution of 30 arc second. Each pixel records a Digital Number (DN) value ranging from 0 to 63. Because the DMSP-OLS data has no onboard calibration, intercalibration of the annual composites is conducted via an empirical method following Elvidge's study (*38*). Using F12 1999 as the reference, the calibration equation in this study is as follows

$$DN_{\text{adjust}} = B \times DN^2 + (1 - 63 \times B) \times DN$$

where DN is the original pixel DN value for each calibrated year, DN_{adjust} is the DN value after calibration, and B is a coefficient obtained by comparing the images of Sicily with F12 1999 based on regression using this equation. We don't use images within the China domain for the calibration because there are no ideal places for the calibration which requires the place with a relatively stable socioeconomic level during the calibration period. The values of B and R^2 for each calibrated year are listed in table S7. For each year, we select the satellites with the highest R^2 to represent the NL distribution in that year.

Determination of NL threshold values

Using the GlobeLand30 and the calibrated NL data, we address the county-level NL threshold values for the year 2010 with the assumption that the fractions of GlobeLand30 urban areas in individual counties are equal to the fractions of areas with NL digital values higher than the threshold values. The urban fractions of the 32 cities derived from the Landsat-based 32 city data are used to determine the historical change of NL threshold values over time. These changes are then applied to other counties of the corresponding provinces to address the NL threshold values and to extract urban areas based on NL distributions. For the years earlier than 1992 when NL data are not available, we assume that within a city area, grids with higher NL values tended to become "urban" earlier than those with lower values historically. Therefore, we use the NL distribution in 1992 (the earliest record year) to determine the threshold values and to extract urban areas for preceding years with a similar procedure for the period from 1992 to 2012. For future projection, we assume that grids with higher NL values would become "urban" earlier than those with lower values. Hence, forecasts of urban expansion in 2030 (*29*) and NL distribution in 2012 (the latest record year) are used to determine the threshold values and to extract urban areas with similar procedures for the period from 1992 to 2012. The threshold values between 2012 and 2030 are

calculated by a linear interpolation. The urban areas in 1980, 1990, 2000, 2010, and 2030 are provided in SI data at a 30-arc-second spatial resolution (approximately 1 km).

Supplementary Discussion

Urban boundary definition

In this study, to determine the population distributions, we derived urban areas based on the Landsat images and nighttime light data, which are basically the "build-up areas" and are different from the urban area defined by administrative boundaries. We chose satellite-based urban area instead of administrative-boundary-based one due to several reasons. First, the urban area defined by administrative boundary cannot reflect the accurate dynamics of urban expansion over time. Fig. S11 shows the temporal trends of total urban area defined by administrative boundaries and the satellite built-up area derived in this study. Historically, the administrative-boundary-based urban area varied widely and did not show a consistently increasing trend over time. This is because the criteria defining urban administrative boundary has been changed. Urban area defined by inconsistent criteria cannot be used to reflect the true urban expansion and to spatially allocate urban population. Second, the administrative-boundary-based urban area is larger than the satellite-based one because there are a large proportion of areas within the administrative boundary, especially in the 1990s, that do not have construction and are not inhabited by residents. Using satellite-based built-up area to allocate urban population is a more accurate and feasible way to obtain spatial distribution of urban population. Several previous studies have discussed in detail about the different criteria applied in different census periods (*64*, *65*). Based on these studies, we adjusted the urban population in the third, fourth, and fifth census data to maintain consistent criteria with the sixth census data (*65*).

table S1. Description of the nine factors affecting emission, air quality, and population health associated with RTC.

NO.	Description	Simulation procedure
N1	Population growth	On the basis of 1980 simulation, total population increases to that in 2010 without change in urbanization rate. The grid population densities increase accordingly and proportionally, and thus the relative distribution is the same as that in 1980. Other aspects such as per-capita emissions remain the same as in 1980. Consequently, the emission amounts and intensity from RTC increase along with population increase.
N2	Increase in RTC energy use	On the basis of N1, per-capita RTC energy consumption increases to that in 2010, by county, in terms of total thermal amount consumed. The energy structures remain the same as that in 1980. Therefore, the emissions are increased along with the increase in energy consumption, but the relative contributions of individual fuel types are unchanged.
N3	Change in energy mix due to improvement in living conditions	On the basis of N2, the energy structures are upgraded to those in 2010 by county. Consequently, the emissions of most pollutants are reduced by this factor.
N4	Decrease in emission factors due to technology development	On the basis of N3, the *EF* values decrease to the levels of 2010 based on the technology transition. Consequently, emissions are further reduced.
U1	Relocation of the registered migrants (NUs)	On the basis of N4, migration of NUs is introduced by changing the NU distribution to 2010. The per-capita consumption of NUs remains the same as that of rural population (RRs) in N4. Mostly, this factor leads to the change of emission spatial distributions rather than of emission amounts, but if migration occurs across regions with different power grids, the emissions from electricity consumption will be changed as a result of the difference in *EF* between power grids.
U2	Shift in energy mix of the NUs	On the basis of U1, the energy consumption and structures of NUs are upgraded from rural to urban patterns.
U3	Relocation of the unregistered migrants (MUs)	On the basis of U2, and similarly to U1, migration of MUs is introduced. The per-capita consumption of MUs remains the same as RRs in U2.
U4	Shift in energy mix of the MUs	On the basis of U3, the energy consumption and structures of MUs are changed from those of RRs to MUs.
U5	Urban sprawl	On the basis of U4, urban areas are extended from the 1980 pattern to the 2010 pattern.

table S2. Information on the sector, fuel type, and EF analysis procedure for RTC energy consumption.

<table>
<tr><th>Sector</th><th>Fuel Type</th><th>Subtype</th><th>Procedure for emission factor (EF) analysis</th></tr>
<tr><td rowspan="13">Residential Sector</td><td rowspan="4">Coal</td><td>Raw coal</td><td rowspan="12">For each compound:
1. Consistent EF values for individual subtypes derived from EF database of PKU-inventory and other literatures;
2. Collection of time trends of subtype proportions from “China Energy Statistical Yearbook” (45) and “China Rural Energy Yearbook” (17);
3. Filling up historical missing data and future prediction using technology split method.</td></tr>
<tr><td>Washed coal</td></tr>
<tr><td>Briquettes</td></tr>
<tr><td>Coke</td></tr>
<tr><td rowspan="4">Oil</td><td>Gasoline</td></tr>
<tr><td>Fuel oil</td></tr>
<tr><td>Diesel</td></tr>
<tr><td>LPG</td></tr>
<tr><td rowspan="2">Gas</td><td>Natural gas</td></tr>
<tr><td>Coal gas</td></tr>
<tr><td rowspan="5">Biomass</td><td>Straw (improved)</td></tr>
<tr><td>Straw (traditional)</td></tr>
<tr><td>Wood (improved)</td></tr>
<tr><td>Wood (traditional)</td></tr>
<tr><td>Biogas</td></tr>
<tr><td rowspan="3">Electricity</td><td>Coal fired</td><td>Time trends derived from EF database of PKU-inventory and literature information (8, 47-50, 52, 53)</td></tr>
<tr><td>Oil fired</td><td>Constant values for individual compounds</td></tr>
<tr><td>Gas fired</td><td>Constant values for individual compounds</td></tr>
<tr><td>Heat</td><td></td><td>The same EFs as electricity (combining coal, oil, and gas)</td></tr>
<tr><td rowspan="2">Transportation (private cars and public transit buses)</td><td rowspan="2">Oil</td><td>Gasoline</td><td rowspan="2">Time trends of EFs derived from EF database of PKU-inventory and literature information (8, 47, 49, 59, 52, 53, 63)</td></tr>
<tr><td>Diesel</td></tr>
</table>

table S3. Urban and rural energy empirical models for different fuel types.

Fuel type	Urban/Rural	Model
Electricity	Urban	$y = 0.115 - 2.94 \times \left[1 - \exp\left(-0.172 \times \left\|x - 5.45\right\|^{1.526}\right)\right] - 0.837 \times \left(P_{ele} - mP_{ele}\right) + 0.00623 \times fs - 0.0859 \times hs$
	Rural	$y = 0.597 - 3.76 \times \left[1 - \exp\left(-6.82 \times 10^{-33} \times \left\|x - 26.8\right\|^{23.36}\right)\right] - 0.0510 \times hs - 0.000361 \times den$
Oil & Gas	Urban	$y = -0.348 - 1.41 \times \left[1 - \exp\left(-1.21 \times 10^{-52} \times \left\|x - 24.4\right\|^{39.16}\right)\right] + 0.404 \times \left[1 - \exp\left(-3.32 \times pr_{og}{}^{1.003}\right)\right]$
	Rural	$y = -0.692 - 0.219 - 2.57 \times \left[1 - \exp\left(-7.05 \times 10^{-64} \times \left\|x - 20.9\right\|^{50.70}\right)\right] - 0.0072 \times fs$
Heat	Urban	$y = -12.22 - 1.13 \times \left[1 - \exp\left(-1.64 \times 10^{-47} \times \left\|x - 13.2\right\|^{45.74}\right)\right] - 1.8 \times 10^{-5} \times den_{pw} + 0.02 \times fs - 2.65 \times \left[1 - \exp\left(-1.91 \times 10^{-2} \times \left\|hdd - 13.2\right\|^{0.764}\right)\right]$
Solid Fuel	Urban	$y = -0.822 - 1.14 \times \left[1 - \exp\left(-2.02 \times 10^{-35} \times \left\|x + 12.8\right\|^{28.63}\right)\right] - 0.0046 \times fs + 1.02 \times \left[1 - \exp\left(-6.94 \times 10^{-2} \times hdd^{0.291}\right)\right]$
	Rural	$y = -0.445 - 9321.52 \times \left[1 - \exp\left(-1.55 \times 10^{-5} \times \left\|x - 3.3\right\|^{1.983}\right)\right] - 0.00033 \times den - 0.026 \times hs - 0.0546 \times \left[1 - \exp\left(0.785 \times hdd^{0.1252}\right)\right]$

Variables:

y: log(E_{cap}), log(tce/person/year)

x: log(GDP_{cap}), log(dollar/person/year)

Adjusted factors:

P_{ele}: electricity price, Yuan/(kw•h)

mP_{ele}: national average electricity price, Yuan/(kw•h)

fs: per-capita floor space, m^2/person

hs: household size, person/household

den: spatial average population density, person/km^2

den_{pw}: population-weighted average population density, person/km^2

pr_{og}: per-capita oil and gas production, tce/person

hdd: heating degree day, ℃•day

table S4. Expected values of EFs for various compounds and sources in China in 1980, 1990, 2000, 2010, and 2030. Units: g compound/GJ

Compound	Year	Residential						Traffic
		Coal	Oil	Gas	Biomass	Electricity	Heat	Oil
CO_2	1980	7.84×10^{4}	6.28×10^{4}	5.56×10^{4}	1.12×10^{5}	1.75×10^{5}	1.29×10^{5}	7.42×10^{4}
	1990	7.85×10^{4}	6.38×10^{4}	5.56×10^{4}	1.12×10^{5}	2.15×10^{5}	1.29×10^{5}	7.39×10^{4}
	2000	7.98×10^{4}	6.36×10^{4}	5.56×10^{4}	1.12×10^{5}	2.03×10^{5}	1.29×10^{5}	7.41×10^{4}
	2010	7.97×10^{4}	6.62×10^{4}	5.56×10^{4}	1.12×10^{5}	1.98×10^{5}	1.29×10^{5}	7.44×10^{4}
	2030	7.98×10^{4}	6.64×10^{4}	5.56×10^{4}	1.12×10^{5}	1.26×10^{5}	1.29×10^{5}	7.45×10^{4}
CO	1980	4.95×10^{3}	2.53×10^{2}	1.13×10^{1}	5.92×10^{3}	3.88×10^{2}	2.85×10^{2}	4.94×10^{3}
	1990	5.10×10^{3}	2.85×10^{2}	1.13×10^{1}	5.90×10^{3}	3.04×10^{2}	1.82×10^{2}	4.95×10^{3}
	2000	5.25×10^{3}	2.78×10^{2}	1.13×10^{1}	5.76×10^{3}	1.87×10^{2}	1.18×10^{2}	3.46×10^{3}
	2010	5.74×10^{3}	4.24×10^{2}	1.13×10^{1}	5.53×10^{3}	1.32×10^{2}	8.60×10^{1}	1.69×10^{3}
	2030	5.69×10^{3}	4.38×10^{2}	1.13×10^{1}	5.13×10^{3}	5.07×10^{1}	5.18×10^{1}	7.75×10^{2}
CH_4	1980	3.00×10^{2}	1.04×10^{1}	4.74×10^{0}	1.81×10^{2}	3.87×10^{1}	2.85×10^{1}	2.45×10^{1}
	1990	3.00×10^{2}	1.04×10^{1}	4.74×10^{0}	2.38×10^{2}	4.36×10^{1}	2.61×10^{1}	1.98×10^{1}
	2000	3.00×10^{2}	1.04×10^{1}	4.74×10^{0}	2.67×10^{2}	2.66×10^{1}	1.68×10^{1}	1.01×10^{1}
	2010	3.00×10^{2}	1.04×10^{1}	4.74×10^{0}	2.66×10^{2}	1.67×10^{1}	1.09×10^{1}	5.50×10^{0}
	2030	3.00×10^{2}	1.04×10^{1}	4.74×10^{0}	2.65×10^{2}	4.43×10^{0}	4.53×10^{0}	1.36×10^{0}
N_2O	1980	8.70×10^{1}	6.00×10^{1}	3.00×10^{3}	7.51×10^{0}	1.79×10^{1}	1.32×10^{1}	8.51×10^{0}
	1990	8.70×10^{1}	6.00×10^{1}	3.00×10^{3}	7.51×10^{0}	2.02×10^{1}	1.21×10^{1}	7.47×10^{0}
	2000	8.70×10^{1}	6.00×10^{1}	3.00×10^{3}	7.52×10^{0}	1.23×10^{1}	7.80×10^{0}	7.19×10^{0}
	2010	8.70×10^{1}	6.00×10^{1}	3.00×10^{3}	7.54×10^{0}	7.74×10^{0}	5.03×10^{0}	3.15×10^{0}
	2030	8.70×10^{1}	6.00×10^{1}	3.00×10^{3}	7.54×10^{0}	2.05×10^{0}	2.10×10^{0}	1.66×10^{0}
Hg	1980	1.10×10^{2}	7.57×10^{7}	1.26×10^{3}	9.85×10^{4}	1.36×10^{2}	9.99×10^{3}	3.71×10^{5}
	1990	1.14×10^{2}	7.68×10^{7}	1.26×10^{3}	9.87×10^{4}	1.57×10^{2}	9.38×10^{3}	4.39×10^{5}
	2000	1.15×10^{2}	7.66×10^{7}	1.26×10^{3}	9.83×10^{4}	1.36×10^{2}	8.62×10^{3}	4.03×10^{5}
	2010	1.25×10^{2}	8.14×10^{7}	1.26×10^{3}	9.79×10^{4}	1.18×10^{2}	7.65×10^{3}	2.95×10^{5}
	2030	1.24×10^{2}	8.18×10^{7}	1.26×10^{3}	9.81×10^{4}	2.71×10^{3}	2.78×10^{3}	2.61×10^{5}
NMVOC	1980	2.67×10^{2}	3.31×10^{0}	2.11×10^{0}	3.08×10^{2}	4.42×10^{1}	3.26×10^{1}	2.53×10^{2}
	1990	2.67×10^{2}	3.31×10^{0}	2.11×10^{0}	4.04×10^{2}	4.99×10^{1}	2.98×10^{1}	2.02×10^{2}
	2000	2.67×10^{2}	3.31×10^{0}	2.11×10^{0}	4.53×10^{2}	3.05×10^{1}	1.93×10^{1}	1.04×10^{2}
	2010	2.67×10^{2}	3.31×10^{0}	2.11×10^{0}	4.52×10^{2}	1.91×10^{1}	1.24×10^{1}	5.73×10^{1}
	2030	2.67×10^{2}	3.31×10^{0}	2.11×10^{0}	4.49×10^{2}	5.06×10^{0}	5.18×10^{0}	1.42×10^{1}
SO_2	1980	5.00×10^{2}	2.52×10^{1}	7.45×10^{0}	2.50×10^{1}	2.41×10^{3}	1.77×10^{3}	8.27×10^{1}
	1990	5.00×10^{2}	3.77×10^{1}	7.45×10^{0}	2.50×10^{1}	2.71×10^{3}	1.62×10^{3}	7.30×10^{1}
	2000	5.00×10^{2}	3.49×10^{1}	7.45×10^{0}	2.50×10^{1}	1.66×10^{3}	1.05×10^{3}	1.68×10^{1}
	2010	5.00×10^{2}	9.15×10^{1}	7.45×10^{0}	2.51×10^{1}	1.04×10^{3}	6.76×10^{2}	4.13×10^{0}
	2030	5.00×10^{2}	9.70×10^{1}	7.45×10^{0}	2.51×10^{1}	2.75×10^{2}	2.82×10^{2}	2.18×10^{0}

table S4. (continued)

Compound	Year	Residential						Traffic
		Coal	Oil	Gas	Biomass	Electricity	Heat	Oil
NO_X	1980	6.60×10^{1}	2.94×10^{1}	5.44×10^{1}	8.83×10^{1}	8.79×10^{2}	6.47×10^{2}	4.38×10^{2}
	1990	6.60×10^{1}	3.00×10^{1}	5.44×10^{1}	8.82×10^{1}	9.90×10^{2}	5.93×10^{2}	3.85×10^{2}
	2000	6.60×10^{1}	2.99×10^{1}	5.44×10^{1}	8.84×10^{1}	6.05×10^{2}	3.82×10^{2}	3.71×10^{2}
	2010	6.60×10^{1}	3.29×10^{1}	5.44×10^{1}	8.86×10^{1}	3.79×10^{2}	2.47×10^{2}	1.62×10^{2}
	2030	6.60×10^{1}	3.32×10^{1}	5.44×10^{1}	8.85×10^{1}	1.00×10^{2}	1.03×10^{2}	8.54×10^{1}
OC	1980	2.25×10^{2}	2.13×10^{0}	3.54×10^{2}	2.26×10^{2}	1.65×10^{1}	1.22×10^{1}	4.72×10^{1}
	1990	2.32×10^{2}	2.69×10^{0}	3.54×10^{2}	2.26×10^{2}	8.69×10^{0}	5.20×10^{0}	3.94×10^{1}
	2000	2.26×10^{2}	2.57×10^{0}	3.54×10^{2}	2.17×10^{2}	3.27×10^{0}	2.07×10^{0}	1.97×10^{1}
	2010	2.43×10^{2}	5.14×10^{0}	3.54×10^{2}	2.04×10^{2}	1.71×10^{0}	1.11×10^{0}	1.03×10^{1}
	2030	2.40×10^{2}	5.39×10^{0}	3.54×10^{2}	1.82×10^{2}	7.71×10^{1}	7.89×10^{1}	2.51×10^{0}
BC	1980	1.24×10^{2}	2.33×10^{0}	5.48×10^{1}	7.78×10^{1}	3.49×10^{0}	2.57×10^{0}	1.18×10^{2}
	1990	1.28×10^{2}	2.47×10^{0}	5.48×10^{1}	7.80×10^{1}	2.47×10^{0}	1.48×10^{0}	9.06×10^{1}
	2000	1.26×10^{2}	2.44×10^{0}	5.48×10^{1}	7.74×10^{1}	1.34×10^{0}	8.48×10^{1}	4.74×10^{1}
	2010	1.37×10^{2}	3.04×10^{0}	5.48×10^{1}	7.67×10^{1}	1.18×10^{0}	7.65×10^{1}	2.77×10^{1}
	2030	1.36×10^{2}	3.10×10^{0}	5.48×10^{1}	7.70×10^{1}	6.24×10^{1}	6.39×10^{1}	6.97×10^{0}
TSP	1980	6.57×10^{2}	1.15×10^{1}	2.78×10^{0}	7.38×10^{2}	2.71×10^{3}	2.00×10^{3}	2.48×10^{2}
	1990	6.77×10^{2}	1.22×10^{1}	2.78×10^{0}	7.35×10^{2}	1.59×10^{3}	9.50×10^{2}	1.96×10^{2}
	2000	6.89×10^{2}	1.20×10^{1}	2.78×10^{0}	7.05×10^{2}	8.20×10^{2}	5.19×10^{2}	1.01×10^{2}
	2010	7.51×10^{2}	1.49×10^{1}	2.78×10^{0}	6.56×10^{2}	6.29×10^{2}	4.09×10^{2}	5.67×10^{1}
	2030	7.44×10^{2}	1.51×10^{1}	2.78×10^{0}	5.78×10^{2}	3.36×10^{2}	3.44×10^{2}	1.42×10^{1}
PM_{10}	1980	5.98×10^{2}	1.15×10^{1}	2.78×10^{0}	6.95×10^{2}	7.94×10^{2}	5.85×10^{2}	2.30×10^{2}
	1990	6.17×10^{2}	1.22×10^{1}	2.78×10^{0}	6.93×10^{2}	5.46×10^{2}	3.27×10^{2}	1.82×10^{2}
	2000	6.30×10^{2}	1.20×10^{1}	2.78×10^{0}	6.66×10^{2}	3.12×10^{2}	1.97×10^{2}	9.38×10^{1}
	2010	6.87×10^{2}	1.49×10^{1}	2.78×10^{0}	6.23×10^{2}	2.31×10^{2}	1.50×10^{2}	5.26×10^{1}
	2030	6.81×10^{2}	1.51×10^{1}	2.78×10^{0}	5.54×10^{2}	9.93×10^{1}	1.02×10^{2}	1.31×10^{1}
$PM_{2.5}$	1980	4.63×10^{2}	1.15×10^{1}	2.78×10^{0}	6.63×10^{2}	3.69×10^{2}	2.72×10^{2}	2.10×10^{2}
	1990	4.78×10^{2}	1.22×10^{1}	2.78×10^{0}	6.61×10^{2}	2.76×10^{2}	1.65×10^{2}	1.66×10^{2}
	2000	4.96×10^{2}	1.20×10^{1}	2.78×10^{0}	6.38×10^{2}	1.60×10^{2}	1.01×10^{2}	8.57×10^{1}
	2010	5.42×10^{2}	1.49×10^{1}	2.78×10^{0}	6.00×10^{2}	1.14×10^{2}	7.40×10^{1}	4.81×10^{1}
	2030	5.37×10^{2}	1.51×10^{1}	2.78×10^{0}	5.40×10^{2}	4.22×10^{1}	4.32×10^{1}	1.20×10^{1}
NH_3	1980	1.89×10^{1}	0	0.00×10^{0}	4.31×10^{1}	5.40×10^{1}	7.23×10^{1}	1.64×10^{1}
	1990	1.89×10^{1}	0	0.00×10^{0}	5.65×10^{1}	6.09×10^{1}	6.63×10^{1}	1.47×10^{1}
	2000	1.89×10^{1}	0	0.00×10^{0}	6.34×10^{1}	3.72×10^{1}	4.28×10^{1}	7.08×10^{0}
	2010	1.89×10^{1}	0	0.00×10^{0}	6.32×10^{1}	2.33×10^{1}	2.76×10^{1}	3.28×10^{0}
	2030	1.89×10^{1}	0	0.00×10^{0}	6.29×10^{1}	6.18×10^{2}	1.15×10^{1}	7.73×10^{1}

table S5. Emissions of various air pollutants and greenhouse gases from RTC and the contributions to total emissions in China in 2010.

Compound	Emissions from RTC, Gg/year			Total emission, Gg/year	Percentage
	urban	rural	total		
$PM_{2.5}$	1350	5150	6500	14600	44.5%
PM_{10}	1880	5620	7500	22000	34.1%
TSP	3010	6270	9280	46700	19.9%
OC	420	1800	2220	3240	68.5%
BC	340	746	1090	2480	44.0%
SO_2	3630	1820	5450	30800	17.7%
NO_X	1960	1110	3060	20700	14.8%
NMVOC	700	3640	4340	21100	20.6%
NH_3	43	479	522	10900	4.8%
CO	17600	48100	65700	101000	65.0%
Hg	0.0501	0.0348	0.0849	0.538	15.8%
CH_4	524	2361	2885	78200	3.7%
N_2O	36.8	62.3	99.1	1780	5.6%
CO_2	1190000	400000	1590000	9010000	17.6%

Note:

The values of national total emissions of OC, BC, TSP, $PM_{2.5}$ and PM_{10} are derived from PKU-inventory (*8*, *48*, *50*). Other compounds are derived from EDGAR (*55*). For compound of which emissions in 2010 are not available, emissions in the last reported year are used. The emission units in the table is Gg compound/year (e.g., Gg CO_2/year for CO_2).

table S6. Sensitivity of $PM_{2.5}$ (primary + secondary) concentrations to change in emissions of individual pollutants.

Pollutant	$PM_{2.5}$ sensitivities to change in emissions, 100%									
	-100%	-75%	-50%	-25%	-10%	+10%	+25%	+50%	+75%	+100%
BC	-4.8%	-3.6%	-2.4%	-1.3%	-0.4%	0.4%	1.3%	2.5%	3.6%	4.8%
OC	-44.3%	-33.1%	-22.0%	-10.9%	-3.7%	4.4%	11.0%	22.4%	32.5%	43.3%
NH_3	-15.3%	-10.5%	-6.2%	-2.0%	-0.4%	0.5%	2.0%	2.1%	1.9%	2.1%
NO_X	-16.1%	-10.9%	-6.9%	-2.9%	-1.0%	0.9%	2.9%	3.4%	4.4%	5.1%
SO_2	-7.4%	-2.3%	-1.2%	-0.1%	-0.3%	0.8%	0.1%	1.1%	1.6%	2.0%
$uPM_{2.5}$	-24.8%	-18.7%	-12.5%	-6.3%	-2.5%	2.5%	6.3%	12.7%	19.0%	25.4%

Note:

The $PM_{2.5}$ concentrations refer to the average $PM_{2.5}$ exposure concentrations in China. The sensitivity is conducted by a series of 1-month simulations. In each simulation, the total emission of a certain pollutant is changed by a specified factor. Compared to the case without any change in emissions, the percentage of corresponding change in $PM_{2.5}$ exposure concentrations is listed in the table. $uPM_{2.5}$ refers to the unspecified $PM_{2.5}$ which is $PM_{2.5}$ excluding BC and OC.

table S7. DMSP OLS satellite information and regression coefficients for NL intercalibration.

Satellite	Year	B	R^2	If selected (Y)
F10	1992	-5.90×10^{-3}	0.90	Y
	1993	-7.23×10^{-3}	0.93	Y
	1994	-6.74×10^{-3}	0.93	Y
F12	1994	-1.88×10^{-3}	0.91	
	1995	-3.13×10^{-3}	0.92	Y
	1996	-4.23×10^{-3}	0.93	Y
	1997	-2.17×10^{-3}	0.93	Y
	1998	-3.80×10^{-4}	0.96	
	1999	—	—	Y
F14	1997	-9.89×10^{-3}	0.91	
	1998	-9.41×10^{-3}	0.97	Y
	1999	-7.51×10^{-3}	0.97	
	2000	-6.30×10^{-3}	0.93	
	2001	-5.09×10^{-3}	0.94	
	2002	-3.88×10^{-3}	0.92	
	2003	-4.63×10^{-3}	0.94	Y
F15	2000	-9.90×10^{-5}	0.94	Y
	2001	-6.72×10^{-4}	0.96	Y
	2002	7.24×10^{-4}	0.97	Y
	2003	-8.16×10^{-3}	0.93	
	2004	-5.97×10^{-3}	0.95	Y
	2005	-5.25×10^{-3}	0.93	
	2006	-5.63×10^{-3}	0.94	Y
	2007	-6.71×10^{-3}	0.90	
F16	2004	-2.74×10^{-3}	0.89	
	2005	-6.24×10^{-3}	0.94	Y
	2006	-2.45×10^{-3}	0.92	
	2007	8.00×10^{-4}	0.95	Y
	2008	-2.62×10^{-4}	0.94	Y
	2009	-1.43×10^{-3}	0.80	Y
F18	2010	6.19×10^{-3}	0.70	Y
	2011	2.80×10^{-3}	0.90	Y
	2012	4.36×10^{-3}	0.94	Y

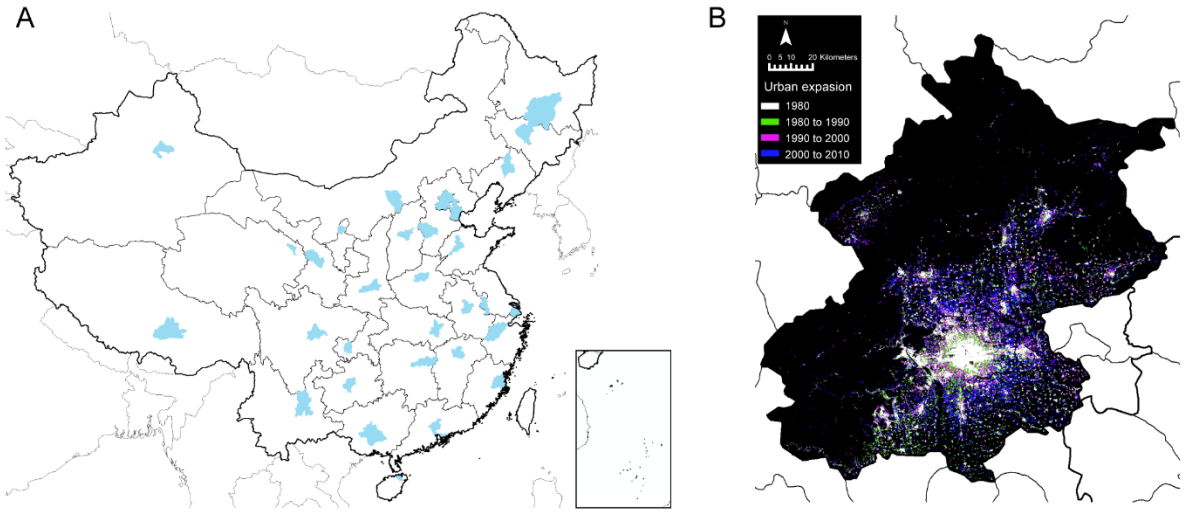

fig. S1. Description of the Landsat-based urban expansion data set. (**A**) The spatial distributions of the administrative areas of the 32 cities. (**B**) Urban expansion in Beijing from 1980 to 2010 derived from Landsat. Detailed information can be found in a previous study (*37*).

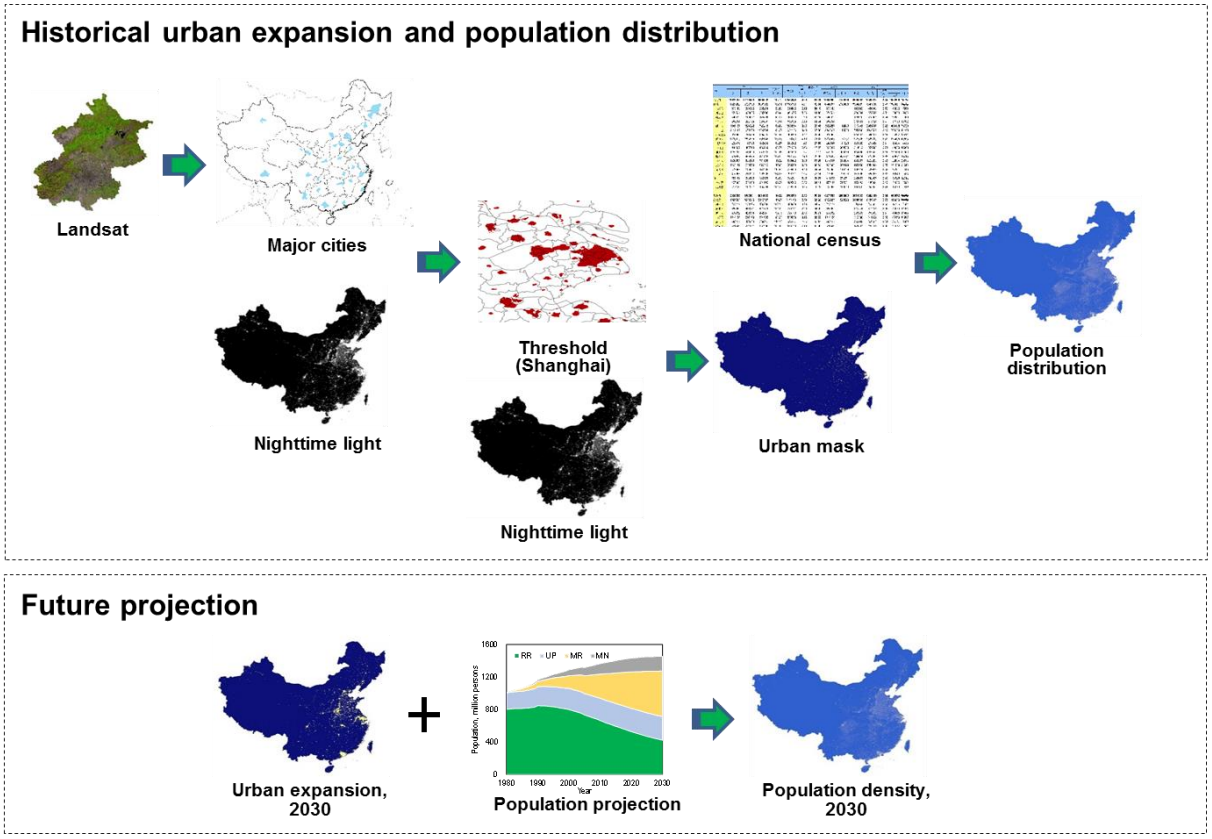

fig. S2. The study framework to address urban expansion and population distribution from 1980 to 2030 in China. (see Materials and Methods for detailed descriptions)

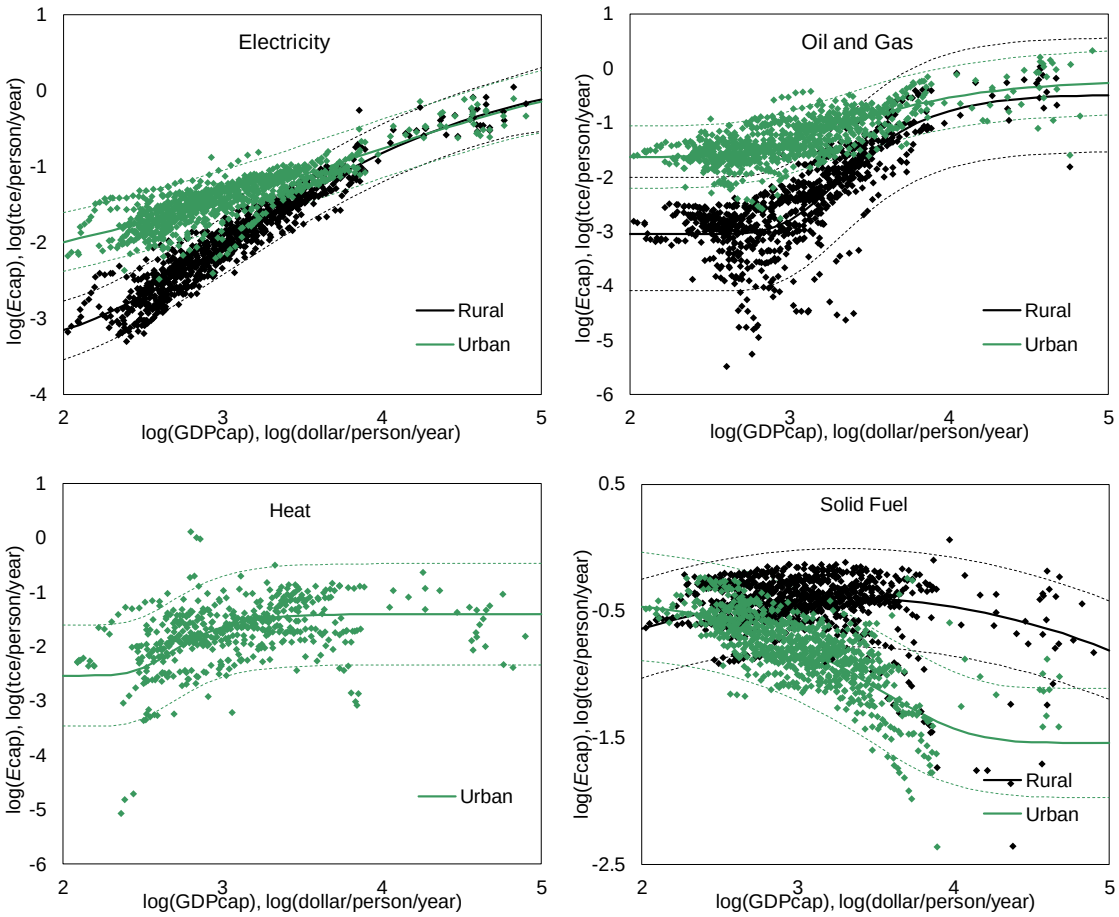

fig. S3. The relation between adjusted E_{cap} and GDP_{cap}. Long-term provincial-level E_{cap} from 1985 to 2012 are plotted against provincial GDP_{cap}. The E_{cap} values were first adjusted by various factors listed in table S3. Green points represent urban data, and black points represent rural data. The solid lines show S-curve regression lines with the dashed lines showing 95% confidence intervals. To address future tendency, data from developed counties are added at higher levels of GDP_{cap}.

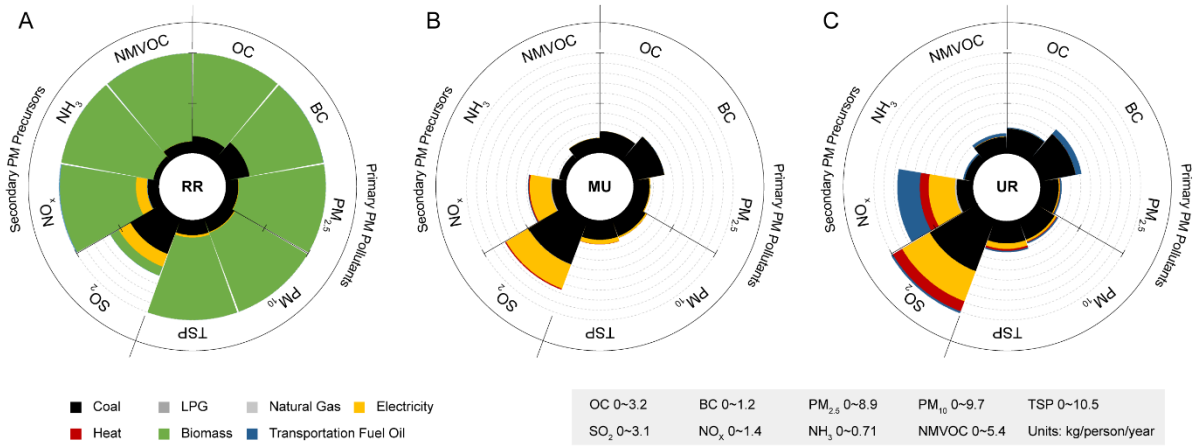

fig. S4. Per-capita RTC emissions in China in 1990. Per-capita RTC emissions of primary PM pollutants and secondary PM precursors of RRs (**A**), MUs (**B**), and URs (**C**) in China by fuel in 1990. The axis ranges of different pollutants are different, as shown in the legend. The per capita emissions shown in the figure are national average levels in 1990.

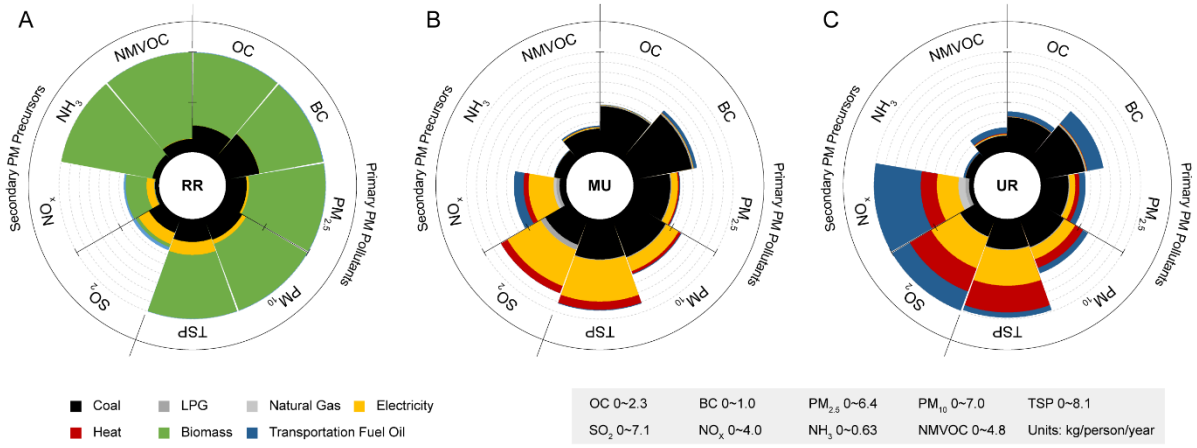

fig. S5. Projected per-capita RTC emissions in China in 2030. Projected per-capita RTC emissions of primary PM pollutants and secondary PM precursors of RRs (**A**), MUs (**B**), and URs (**C**) in China by fuel in 2030. The axis ranges of different pollutants are different, as shown in the legend. The per capita emissions shown in the figure are national averages in 2030.

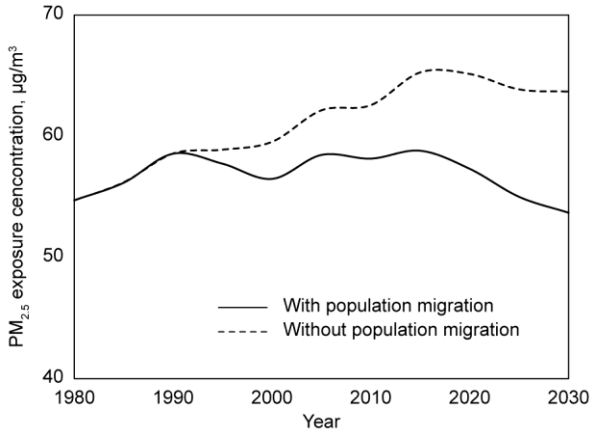

fig. S6. Temporal trends of $PM_{2.5}$ exposure concentrations in China from 1980 to 2030. Temporal trends of $PM_{2.5}$ exposure concentrations over China (**A**) with consideration of rural-urban migration and (**B**) without consideration of rural-urban migration during the period from 1980 to 2030. The temporal trends are only shaped by the changes in RTC sources. Other sources such as industrial and agricultural sources remain unchanged over time.

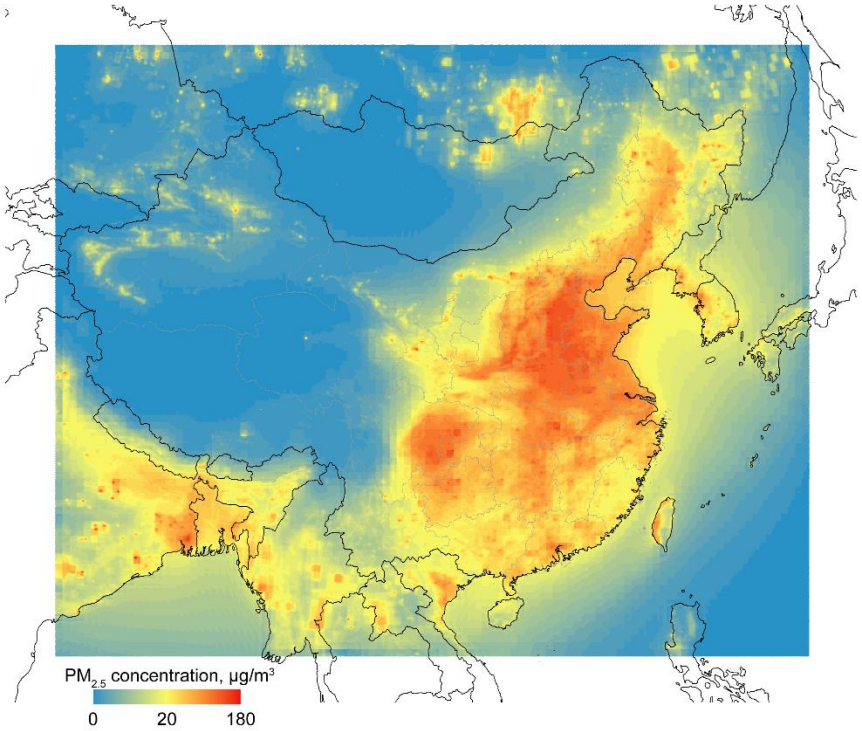

fig. S7. Modeled annual average near-surface $PM_{2.5}$ concentrations in the modeling domain in 2010. The $PM_{2.5}$ concentrations are simulated by the WRF/Chem model coupled with the Gaussian downscaling method. The spatial resolution is 5km × 5km. The concentrations include primary and secondary $PM_{2.5}$ and exclude dust and sea salt.

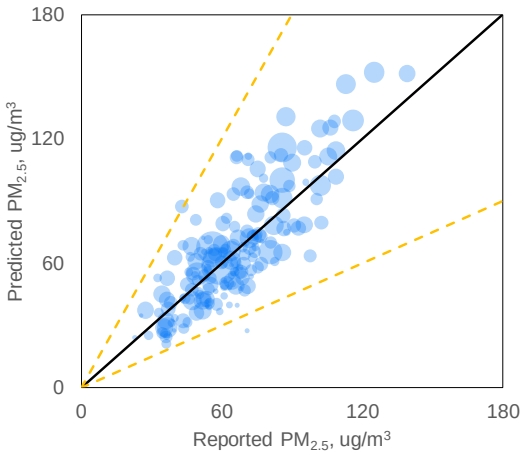

fig. S8. Comparison of annual average $PM_{2.5}$ concentrations between simulation and observation. Downscaled annual average $PM_{2.5}$ concentrations (including dust and sea salt) are plotted against observations in 190 cities reported by the national air quality monitoring network for the 1-year period from September 1st, 2013 to August 31th, 2014 (*25*). Each bubble represents a city. The areas pf the bubbles are proportional to the city population. For cities with more than one site, observed concentrations are averaged. City centers are used to locate the simulation grid cell of the city. The black solid line is the 1:1 line, and the orange dashed lines show the 1:2 and 2:1 lines.

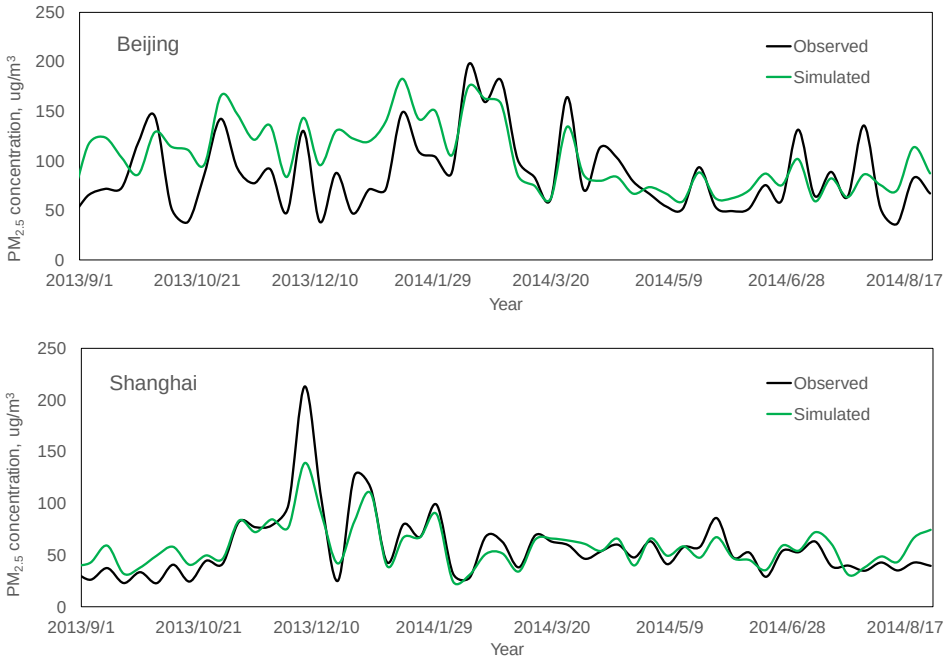

fig. S9. Comparison of time series of $PM_{2.5}$ concentrations between simulation and observation in Beijing and Shanghai. Weekly time series of downscaled $PM_{2.5}$ concentrations (including dust and sea salt) are compared with observations in Beijing and Shanghai reported by the national air quality monitoring network for the period from September 1st, 2013 to August 31th, 2014 (*25*).

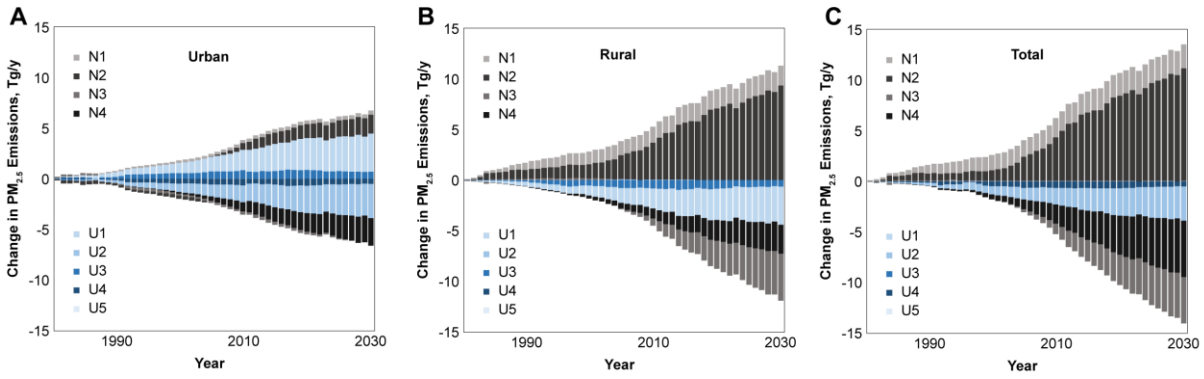

fig. S10. The influences of individual non–migration-related (N1 to N4) and migration-related (U1 to U5) factors on $PM_{2.5}$ emissions in China during the study period. Influence on emissions in urban (**A**), rural (**B**), and total (**C**) areas are illustrated separately.

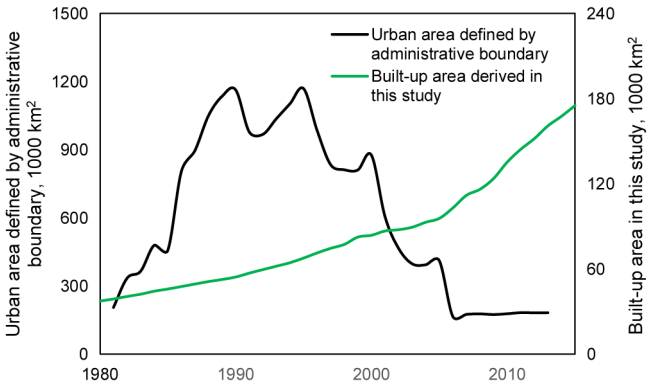

fig. S11. Temporal trends of the national total urban area defined by administrative boundaries (*45*) and the built-up area derived in this study.